

A new technique for the characterization of viscoelastic materials: theory, experiments and comparison with DMA.

Elena Pierro¹, Giuseppe Carbone^{2,3}

¹*Scuola di Ingegneria, Università degli Studi della Basilicata, 85100 Potenza, Italy*

²*Department of Mechanics, Mathematics and Management,
Polytechnic University of Bari, V.le Japigia, 182, 70126, Bari, Italy and*

³*Physics Department M. Merlin, CNR Institute
for Photonics and Nanotechnologies U.O.S. Bari,
via Amendola 173, Bari, 70126, Italy*

Abstract

In this paper we present a theoretical and experimental study aimed at characterizing the hysteretic properties of viscoelastic materials. In the last decades viscoelastic materials have become a reference for new technological applications, which require lightweight, deformable but ultra-tough structures. The need to have a complete and precise knowledge of their mechanical properties, hence, is of utmost importance. The presented study is focused on the dynamics of a viscoelastic beam, which is both experimentally investigated and theoretically characterized by means of an accurate analytical model. In this way it is possible to fit the experimental curves to determine the complex modulus. Our proposed approach enables the optimal fitting of the viscoelastic modulus of the material by using the appropriate number of relaxation times, on the basis of the frequency range considered. Moreover, by varying the length of the beams, the frequency range of interest can be changed/enlarged. Our results are tested against those obtained with a well established and reliable technique as compared with experimental results from the Dynamic Mechanical Analysis (DMA), thus definitively establishing the feasibility, accuracy and reliability of the presented technique.

Part I

Introduction

Recent scientific advancements in field of automotive, electronics, micromechanical systems, pipe technologies, have led to new technologies where the use of lightweight, tough, soft and high deformable materials has become ubiquitous. In this scenario, viscoelastic materials have spread in many different contexts, from seals [1] to bio-inspired adhesives [2–5], because of their superior damping and frictional properties. For an appropriate use of such materials, however, the proper knowledge of their mechanical properties is a basic requirement. Along this line, the most popular technique to characterize the viscoelastic modulus of such materials is the Dynamic Mechanical Analysis (DMA) [7, 8], which allows the measurement of the viscoelastic complex modulus depending on both frequency and temperature. In particular, it consists of imposing a small cyclic strain on a sample and measuring the resulting stress response, or equivalently, imposing a cyclic stress on a sample and measuring the resultant strain response. Nevertheless, such an experimental procedure exhibits different limits (e.g. high frequency characterization is considerably difficult [9–11]) and requires expensive test equipment. In this view, several techniques have been proposed, based on the vibrational response of beam like structures. In Ref. [12], the complex modulus of acoustic materials using a transfer function method of a lumped mechanical model was utilized. In Ref. [13] the response of the endpoint of an impacted beam was measured in terms of displacements, by means of electro-optical transducers, and then an iterative numerical scheme was considered to retrieve the viscoelastic modulus. Other experimental procedures have been recently presented, with the aim of simplifying the setup, as in Ref. [14] where a double pendulum was utilized to excite a viscoelastic sample without any other source of external excitation, and recorded oscillations were induced by gravity. In Ref. [15] a cantilever beam was excited by means of a seismic force, and curve fitting of experimental data with a fractional derivative model was employed to characterize the complex modulus. However, in all the presented works dealing with mechanical characterization of viscoelastic materials, there is no the simultaneous presence of i) a very simple setup, ii) an analytical model to describe the dynamics of the vibrational system considered, and iii) a constitutive model able to accurately capture the behaviour of viscoelastic materials in a wide frequency range. Moving

from these facts, in this paper we present a rigorous easy-to-use approach for determining the viscoelastic modulus, based on the experimental vibrational identification of viscoelastic beams with different lengths. Both a very simple setup is utilized for acquisitions, and an accurate analytical model of the beam are considered to determine the viscoelastic modulus, which takes into account multiple relaxation times of the material. In particular, by properly changing the length of the considered beam, it is possible to broaden the frequency range under analysis, and by selecting the appropriate number of relaxation times it is possible to optimize the fitting procedure. The results presented in this paper show that these two aspects are of pivotal importance to correctly determine the viscoelastic complex modulus, and they open new paths towards challenging further improvements. The paper is organized as follows: at first, the analytical model of a viscoelastic beam dynamics is recalled, then the experimental setup and the data acquisition are explained in detail. Finally, the curve fitting scheme is defined and results are discussed in depth, with particular emphasis on the comparison with DMA results.

I. THEORETICAL MODEL OF THE VISCOELASTIC BEAM DYNAMICS

In this section, we derive the analytical formulation of the viscoelastic beam vibrational response. The main purpose is to get a simple-to-use formula, which can be utilized to characterize the viscoelastic modulus, by fitting the experimental acquisitions. It is known, in particular, that for viscoelastic materials, the stress-strain relation is governed by the following integral [6]

$$\sigma(x, t) = \int_{-\infty}^t G(t - \tau) \dot{\varepsilon}(x, \tau) d\tau \quad (1)$$

where $\dot{\varepsilon}(t)$ is time derivative of the strain, $\sigma(t)$ is the stress, $G(t - \tau)$ is the so called relaxation function. The viscoelastic complex modulus $E(s)$ is closely related to the relaxation function $G(t)$, and the simple equality $E(s) = sG(s)$ exists in the Laplace domain. In this domain, in particular, it is possible to represent the complex modulus $E(s)$ as the following series

$$E(s) = E_0 + \sum_k E_k \frac{s\tau_k}{1 + s\tau_k} \quad (2)$$

which derives from the generalized Maxwell model, consisting of a spring with elastic constant E_0 , that represents the elastic modulus of the material at zero-frequency, and k Maxwell

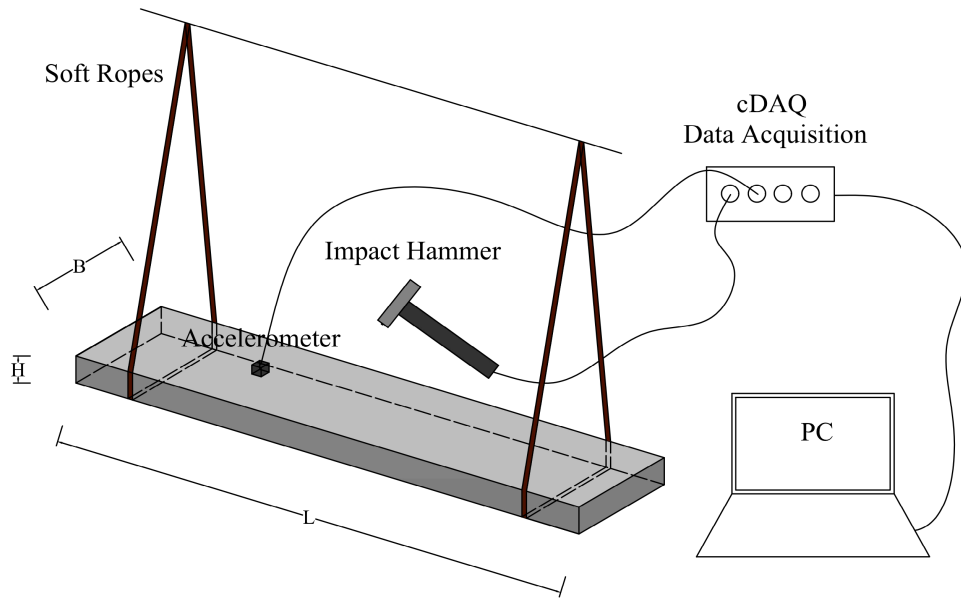


FIG. 1: The schematic of the test rig.

elements connected in parallel, i.e. spring elements characterized by both the relaxation time τ_k and the elastic modulus E_k . By considering the above Eqs.(1)-(2) in the theoretical model utilized to fit the experimental responses of the vibrating beam, it is possible to establish the optimal number of relaxation times to better capture the viscoelastic behaviour in a certain frequency range.

The geometrical characteristics of the beam considered in the present paper are chosen in order to follow the Bernoulli theory of flexural vibrations, i.e. $L \gg W$, $L \gg B$, being L the length of the beam, W and B respectively the width and the thickness of the rectangular cross section.

In particular, by assuming that the transversal displacement $|u(x, t)| \ll L$, it is possible to neglect the contribute of shear stress, which is always very low at the first resonances. The equation of motion can be therefore written as [16]

$$J_{xz} \int_{-\infty}^t E(t - \tau) \frac{\partial^4 u(x, \tau)}{\partial x^4} d\tau + \mu \frac{\partial^2 u(x, t)}{\partial t^2} = f(x, t) \quad (3)$$

being $\mu = \rho A$, ρ the bulk density of the material, $A = WB$ the cross section area, $J_{xz} = (1/12)WB^3$ the moment of inertia, and $f(x, t)$ the generic force acting on the beam. The solution of Eq.(3) can be formulated in terms of the eigenfunctions $\phi_n(x)$ by means of the

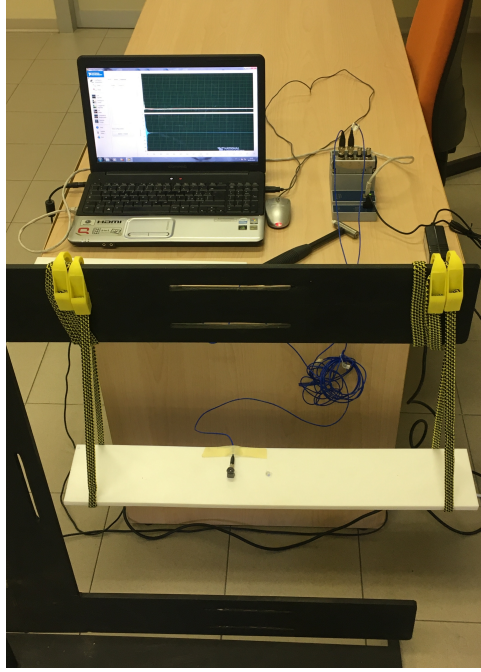


FIG. 2: The experimental setup, consisting of i) the suspended viscoelastic beam (length $L = 60$ [cm]) with a PCB 333B30 ICP accelerometer, glued on the upper surface, ii) the cDAQ-9184 NI data acquiring, iii) the PCB 086C03 ICP Impact Hammer and iv) a portable pc.

decomposition of the system response

$$u(x, t) = \sum_{n=1}^{+\infty} \phi_n(x) q_n(t) \quad (4)$$

It can be shown that the eigenfunctions $\phi_n(x)$ do not change if we consider a viscoelastic material instead of a perfectly elastic one. The eigenfunctions $\phi_n(x)$, in particular, can be calculated by solving the homogeneous problem

$$J_{xz} \int_{-\infty}^t E(t - \tau) \frac{\partial^4 u(x, \tau)}{\partial x^4} d\tau + \mu \frac{\partial^2 u(x, t)}{\partial t^2} = 0 \quad (5)$$

with the opportune boundary conditions. In the Laplace domain, by considering the initial conditions equal to zero, Eq.(5) becomes

$$\phi_{xxxx}(x, s) - \beta_{eq}^4(s) \phi(x, s) = 0 \quad (6)$$

($\phi_x(x, s) = \partial\phi(x, s) / \partial x$) having defined

$$\beta_{eq}^4(s) = -\frac{\mu s^2}{J_{xz} E(s)} = -\frac{\mu s^2}{J_{xz}} C(s) \quad (7)$$

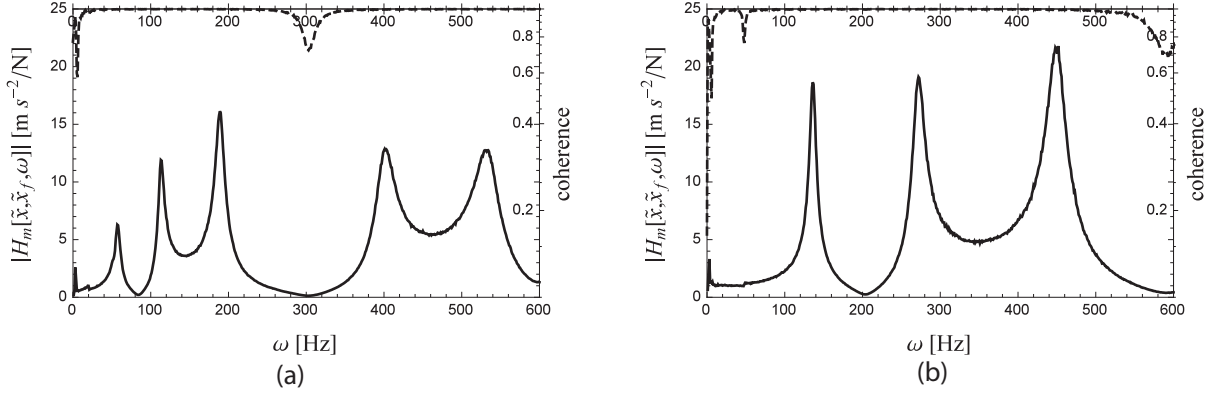


FIG. 3: The measured frequency response functions $H_m(\tilde{x}, \tilde{x}_f, \omega)$ (solid lines) and the coherence (dashed lines), in the range 0 – 600 [Hz], for the beams of length $L = 60$ [cm] (a) and $L = 40$ [cm] (b).

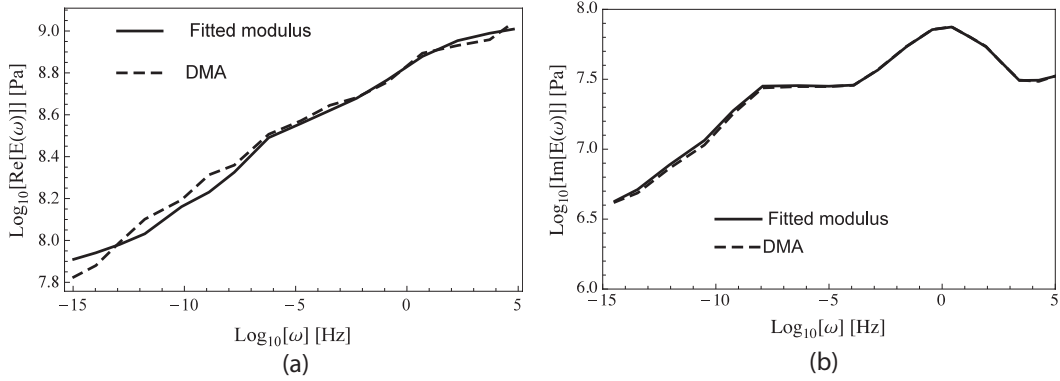


FIG. 4: Master curves of LUBRIFLON (Dixon Resine [19]) at 20°C (dashed lines), fitted by means of Eq.(2) by considering 50 relaxation times (solid lines), as real part $\text{Re}[E(\omega)]$ (a) and imaginary part $\text{Im}[E(\omega)]$ (b) of the viscoelastic modulus $E(\omega)$.

with $C(s) = 1/E(s)$ the compliance of the viscoelastic material. In the present study, we determine experimentally the beam response when it is suspended at a fixed frame, in the so called "free-free" boundary condition. From a mathematical point of view, this set-up

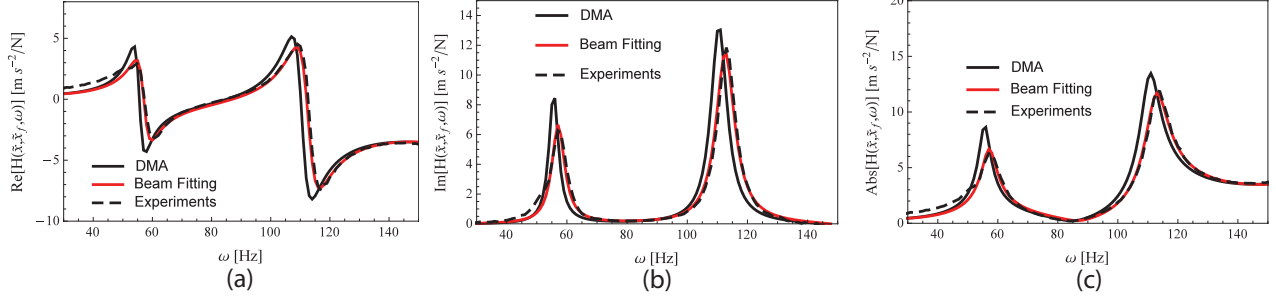


FIG. 5: The comparison between the measured FRF $H_m(\tilde{x}, \tilde{x}_f, \omega)$ (black dashed lines) and the theoretical FRF $H_{th}(\tilde{x}, \tilde{x}_f, \omega)$, obtained through beam-best fitting (red lines) and DMA data (black solid lines), for the beam of length $L = 60$ [cm]. Curves are shown in terms of real part (a), imaginary part (b) and absolute value (c) of the FRFs.

corresponds to the following mathematical conditions

$$\begin{aligned}
 \phi_{xx}(0, s) &= 0 \\
 \phi_{xxx}(0, s) &= 0 \\
 \phi_{xx}(L, s) &= 0 \\
 \phi_{xxx}(L, s) &= 0
 \end{aligned} \tag{8}$$

From the solution of Eq.(6), which is of the following type

$$\phi(x, s) = W_1 \cos[\beta_{eq}(s)x] + W_2 \sin[\beta_{eq}(s)x] + W_3 \cosh[\beta_{eq}(s)x] + W_4 \sinh[\beta_{eq}(s)x] \tag{9}$$

it is possible to derive the well known equation

$$[1 - \cos(\beta_{eq}L) \cosh(\beta_{eq}L)] = 0 \tag{10}$$

by simply forcing equal to zero the determinant of the system matrix obtained from Eqs.(8). Let us observe that the solutions $\beta_n L = c_n$ of Eq.(10) are the same of the perfectly elastic case, and can be substituted in Eq.(7) to calculate the complex conjugate eigenvalues s_n corresponding to the n modes of the beam, and the real poles s_k related to the material viscoelasticity [17, 18]. Furthermore, by means of the solutions $\beta_n L = c_n$ of Eq.(10), it is possible to derive the following eigenfunctions $\phi_n(x)$

$$\phi_n(x) = \cosh(\beta_n x) + \cos(\beta_n x) - \frac{\cosh(\beta_n L) - \cos(\beta_n L)}{\sinh(\beta_n L) - \sin(\beta_n L)} [\sinh(\beta_n x) + \sin(\beta_n x)] \tag{11}$$

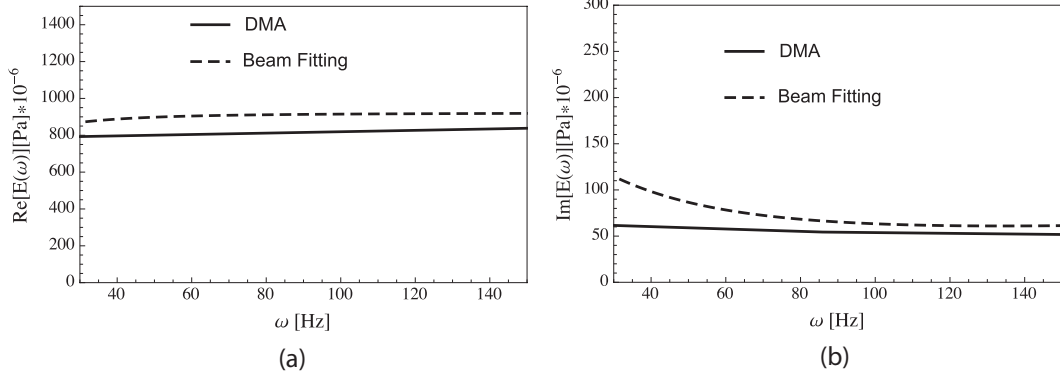


FIG. 6: The real part (a) and the imaginary part (b) of the viscoelastic modulus $E(\omega)$, obtained by fitting the vibrational response of the beam with $L = 60$ [cm] (dashed line) and by DMA (solid line), in the frequency range 30 – 150 [Hz].

which have the same analytical form of the eigenfunctions of a beam made of an elastic material. In particular, these functions follow the orthogonality condition

$$\frac{1}{L} \int_0^L \phi_n(x) \phi_m(x) dx = \delta_{nm} \quad (12)$$

being δ_{nm} the Kronecker delta function, as well as from Eq.(6) one gets

$$\frac{1}{L} \int_0^L (\phi_n)_{xxxx}(x) \phi_m(x) dx = \frac{1}{L} \int_0^L \phi_n(x) \beta_n^4 \phi_m(x) dx = \delta_{nm} \beta_n^4 \quad (13)$$

Through the above Eqs.(12)-(13), and by defining the projected solution $u_m(t)$ on the m_{th} eigenfunction $\phi_m(x)$ as

$$u_m(t) = \langle u(x, t) \phi_m(x) \rangle = \frac{1}{L} \int_0^L u(x, t) \phi_m(x) dx \quad (14)$$

it is possible to rewrite Eq.(3), after simple calculations, as following

$$\mu \ddot{q}_n(t) + J_{xz} \beta_n^4 \int_{-\infty}^t E(t - \tau) q_n(\tau) d\tau = f_n(t) \quad (15)$$

where $f_n(t) = \frac{1}{L} \int_0^L f(x, t) \phi_n(x) dx$ is the projected force. The Laplace Transform of Eq.(15), with initial conditions equal to zero, is

$$\mu s^2 Q_n(s) + J_{xz} \beta_n^4 E(s) Q_n(s) = F_n(s) \quad (16)$$

and therefore the system response, defined in Eq.(4), becomes in the Laplace domain

$$U(x, s) = \sum_{n=1}^{+\infty} \phi_n(x) Q_n(s) = \sum_{n=1}^{+\infty} \phi_n(x) \frac{F_n(x, s)}{\mu s^2 + J_{xz} \beta_n^4 E(s)} \quad (17)$$

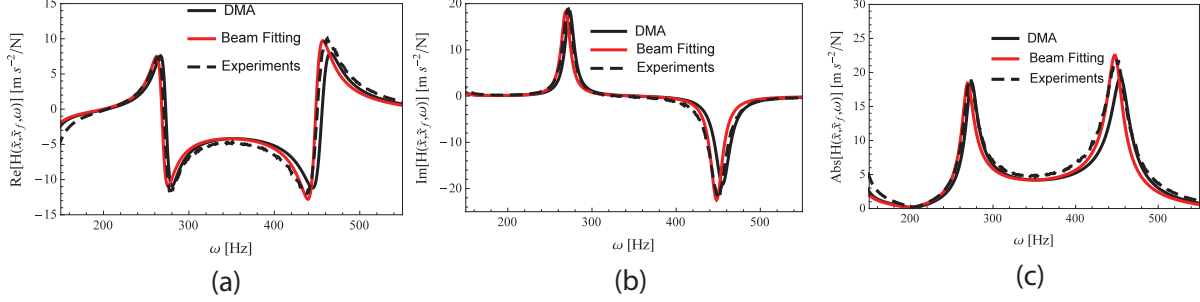


FIG. 7: The comparison between the measured FRF $H_m(\tilde{x}, \tilde{x}_f, \omega)$ (black dashed lines) and the theoretical FRF $H_{th}(\tilde{x}, \tilde{x}_f, \omega)$, obtained through beam-best fitting (red lines) and DMA data (black solid lines), for the beam of length $L = 40$ [cm]. Curves are shown in terms of real part (a), imaginary part (b) and absolute value (c) of the FRFs.

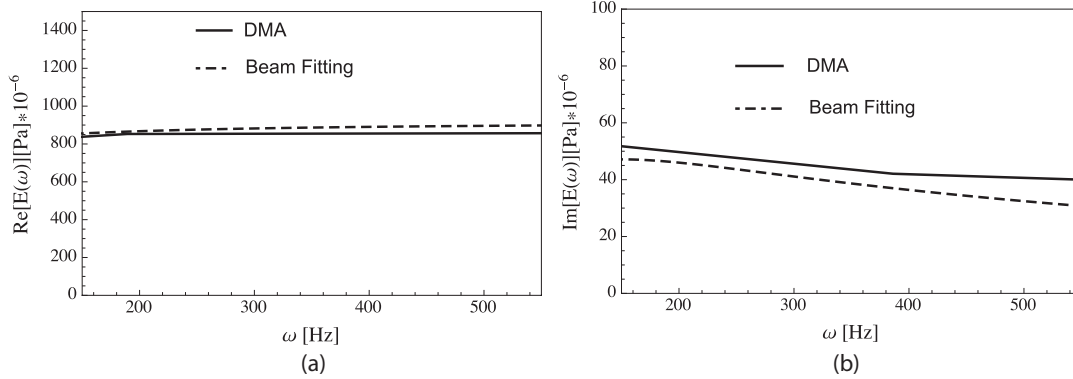


FIG. 8: The real part (a) and the imaginary part (b) of the viscoelastic modulus $E(\omega)$, obtained by fitting the vibrational response of the beam with $L = 40$ [cm] (dashed line) and by DMA (solid line), in the frequency range 150 – 550 [Hz].

For the scope of our investigation, we need to further modify Eq.(17). Indeed, we experimentally excite the beam (see Section II) by means of an impact hammer, in the section $x = x_f$, at the instant $t = t_0$. Analytically, this condition is equivalent to consider as forcing term, a Dirac Delta of constant amplitude F_0 , in both the time and the spatial domains $f(x, t) = F_0 \delta(x - x_f) \delta(t - t_0)$, i.e. in the Laplace domain the projected force is $F_n = \int_0^L F_0 \delta(x - x_f) \phi_n(x) dx = F_0 \phi_n(x_f)$. Hence, the analytic response of the beam can be rewritten as

$$U(x, x_f, s) = F_0 \sum_{n=1}^{+\infty} \frac{\phi_n(x) \phi_n(x_f)}{\mu s^2 + J_{xz} \beta_n^4 E(s)} \quad (18)$$

The beam response, derived in the above Eq.(18), can be utilized to determine the viscoelastic modulus $E(s)$, previously defined by Eq.(2). In particular, the following theoretical frequency response function (FRF), can be defined in terms of inertance

$$H_{th}(x, x_f, i\omega) = \frac{A(x, i\omega)}{F_0} = (i\omega)^2 \sum_{n=1}^{+\infty} \frac{\phi_n(x) \phi_n(x_f)}{\mu (i\omega)^2 + J_{xz} \beta_n^4 E(i\omega)} \quad (19)$$

being the acceleration $A(x, i\omega) = U(x, i\omega) (i\omega)^2$. In this way, Eq.(19) can be utilized to fit the experimentally acquired FRF, as discussed in the next Section.

II. EXPERIMENTAL TEST

Two viscoelastic beams made of LUBRIFLON (Dixon Resine [19]), with thickness $B = 1$ [cm], width $W = 10$ [cm], lengths $L = 60$ [cm] and $L = 40$ [cm], were suspended at a fixed frame through soft ropes. Different lengths, in particular, enable to enlarge the frequency range of interest, thus resulting in a better characterization of the material damping properties, as it will be thoroughly discussed in the next Sections. Furthermore, by considering beams with different lengths, it is possible to survey potential peaks suppression or mitigation, according to the theoretical studies previously presented in Ref.[17, 18]. The schematic of the test rig is drawn in Figure 1. The basic experimental setup (laboratory of Applied Mechanics, University of Basilicata, Potenza, Italy), is shown in Figure 2. This kind of setup, which represents the free-free boundary condition, is suitable in order to avoid external influences on damping due to constraints [20], as it happens for example when the beam is clamped. The cDAQ-9184 CompactDAQ (National Instruments) data acquiring has been utilized to collect the time histories, through the NI Sound and Vibration Toolkit included in LabVIEW (National Instruments). The slender beam has been excited in the z -direction through the PCB 086C03 ICP Impact Hammer, and the accelerations have been acquired, in the same direction, by means of a PCB 333B30 ICP Accelerometer. The beam sections chosen for the impacting excitation and for the acceleration acquisitions were respectively $\tilde{x}_f = 0.8L$ and $\tilde{x} = 0.4L$. The motivation behind this choice lies in the fact that, in this way, by properly avoiding the nodal points, the first vibrational modes $\phi_{1,5}(x_f)$ should all be present in the measures FRFs, in the frequency range under analysis. However, it is

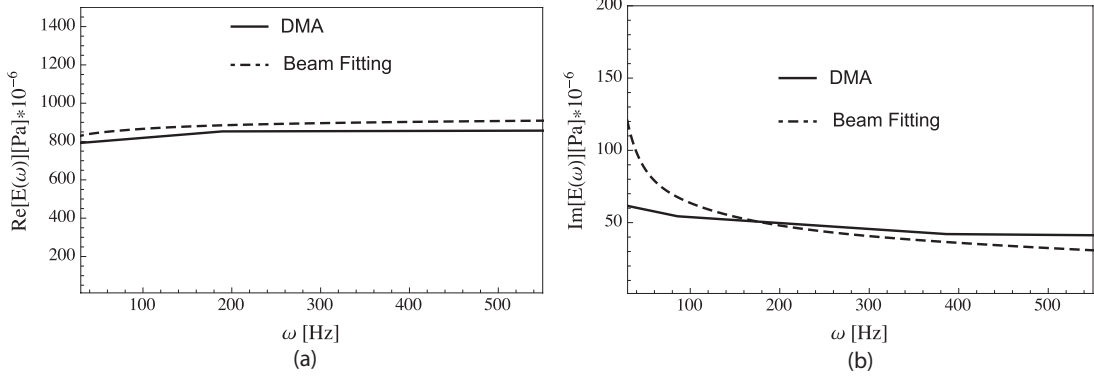


FIG. 9: The real part (a) and the imaginary part (b) of the viscoelastic modulus $E(\omega)$, in the frequency range 30 – 550 [Hz], obtained from DMA (solid line) and by fitting the two moduli determined through the vibrational responses of the two beams with different lengths (dashed line).

expected a mitigation of both the first and fifth peaks, since the section of the input force \tilde{x}_f is close to nodal points for the corresponding two mode shapes.

We acquired a group of 10 time histories, each lasting 1 [s], with sampling frequency $f_s = 25600$ [Hz]. It should be observed that, because of the heavy damped material, the signal decreased to zero at about 1/5 of the acquisition time, so there was no need to apply any windows to time histories. Then, we have calculated the Fast Fourier Transform (FFT) of the ten averaged time histories, for both the accelerations $A(\tilde{x}, \omega)$ and the impacting forces $F(\tilde{x}_f, \omega)$. Finally, the H_1 estimator [21] has been considered to determine the measured frequency response functions $H_m(\tilde{x}, \tilde{x}_f, \omega)$, which are shown in Figure 3, for the beams of length $L = 60$ [cm] (Figure 3-a) and $L = 40$ [cm] (Figure 3-b), in terms of absolute value of the function $H_m(\tilde{x}, \tilde{x}_f, \omega)$ (solid lines), in the frequency range 0 – 600 [Hz]. Moreover, the coherence function [21] (dashed lines) for each acquisition is shown, for the same frequency range. It is possible to observe that, as expected, same resonances moves forward higher frequencies, by decreasing the beam length L . However, in contrast to a perfectly elastic beam, the amplitude of such peaks changes. In particular, the second peak, which is at $\omega \simeq 60$ [Hz] for the beam of length $L = 60$ [cm] (Figure 3-a), moves to $\omega \simeq 120$ [Hz] for the beam with $L = 40$ [cm] (Figure 3-b) and its amplitude increases. This circumstance suggests that the transition region of the material, where damping effects are more significant, should be found at lower frequencies. For both the material and the beam geometry considered in

the present study, a slight mitigation of the resonances can be observed, and not a complete peak suppression [17, 18]. This fact helps in interpreting the nature of the peaks in the frequency range considered, and thus enables us to perform a correct viscoelastic modulus fitting.

III. VISCOELASTIC PARAMETERS IDENTIFICATION

By observing the coherence functions in Figure 3, it is possible to notice that some problems occurred before the second and after the fourth peaks, for both the tests. As previously discussed, this condition could be related to the selected impact section \tilde{x}_f , which is near to the nodal points of both the first and the fifth mode shapes $\phi_{1,5}(x_f)$. Therefore, in order to get the correct information from the experimental data in the fitting procedure, we have considered only the frequency range with maximum coherence, i.e. 30 – 250 [Hz] for the beam with $L = 60$ [cm], and 150 – 500 [Hz] for the beam with $L = 40$ [cm]. In the first case ($L = 60$ [cm]), we have excluded the first peak at $\omega \simeq 20$ [Hz], since it is too near to the zone with low coherence. In the latter case ($L = 40$ [cm]), we have excluded both the first ($\omega \simeq 50$ [Hz]) and the second peak ($\omega \simeq 120$ [Hz]), because of the heavy drop of the coherence in correspondence of the first resonance.

The measured frequency response function $H_m(\tilde{x}, \tilde{x}_f, \omega)$ has been fitted by means of the theoretical FRF $H_{th}(\tilde{x}, \tilde{x}_f, \omega)$ defined in Eq.(19), in which only the viscoelastic modulus $E(\omega)$ is unknown. Hence, we have defined the cost function ϵ_k as the squared difference between the real and imaginary parts of the theoretical $H_{th}(\tilde{x}, \tilde{x}_f, \omega)$ and the measured $H_m(\tilde{x}, \tilde{x}_f, \omega)$ FRFs:

$$\epsilon_k = \sum_{i=n}^m [(\text{Re}[H_{th}(\tilde{x}, \tilde{x}_f, \omega_i)] - \text{Re}[H_m(\tilde{x}, \tilde{x}_f, \omega_i)])^2 + \quad (20)$$

$$+ (\text{Im}[H_{th}(\tilde{x}, \tilde{x}_f, \omega_i)] - \text{Im}[H_m(\tilde{x}, \tilde{x}_f, \omega_i)])^2] \quad (21)$$

The best fit of the theoretical model has been performed by minimizing the above defined cost function ϵ_k , which depends on the number k of relaxation times considered to characterize the viscoelastic modulus $E(\omega)$. In this manner, the viscoelastic modulus $E(\omega)$ (see definition in the Laplace domain in Eq.(2)), can be determined in terms of i) the elastic modulus at zero-frequency E_0 , ii) the relaxation times τ_k , and iii) the correspondent elastic moduli E_k . The fundamental novelty of the presented approach, with respect to the other

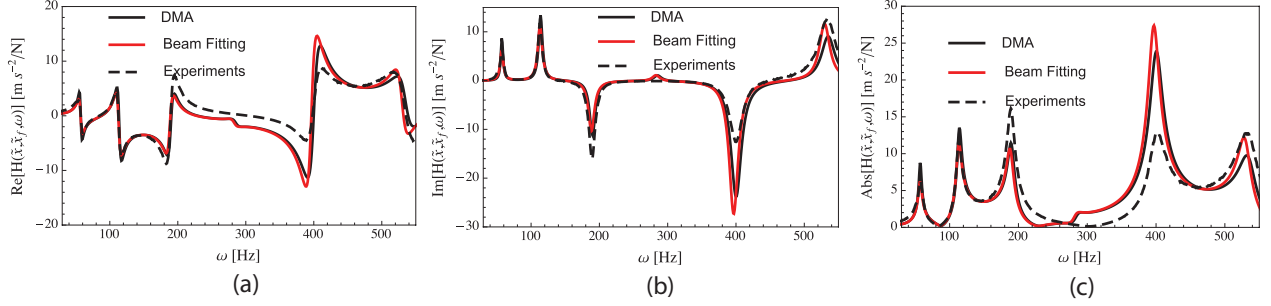


FIG. 10: The comparison between the measured FRF $H_m(\tilde{x}, \tilde{y}, \omega)$ (black dashed lines) and the theoretical FRF $H_{th}(\tilde{x}, \tilde{y}, \omega)$, obtained through beam-best fitting (red lines) and DMA data (black solid lines), for the beam with $L = 60$ [cm], in the range $30 - 550$ [Hz], in terms of real part (a), imaginary part (b) and absolute value (c) of the FRFs.

similar vibration-based procedures presented in literature (e.g. [15]), consists in the fitting method, which can be optimized by properly choosing the number k of relaxation times, to correctly fit the beam dynamic response. This number, in particular, is influenced by the width of the frequency band considered, and by the amount of damping present in a certain frequency range.

With the aim of assessing the presented technique, we have also experimentally characterized our viscoelastic material through a Dynamic Mechanical Analyzer - MCR 702 MultiDrive - Anton Paar GmbH (Tribolab, Politecnico di Bari, Bari, Italy). However, the DMA approach is different, since the viscoelastic modulus $E(\omega)$ is directly measured by considering the stress - strain relation shown in the Eq.(1). Therefore, in order to define a frequency response function based on DMA results, we need an analytical form of the viscoelastic modulus $E(\omega)$ to be considered in Eq.(19). Hence, we have fitted the experimental viscoelastic modulus $E(\omega)$ measured with DMA, by means of Eq.(2). In Figure 4 it is shown the good correlation between the experimental master curve and the fitted complex modulus, for both the real part (Figure 4-a) and the imaginary part (Figure 4-b).

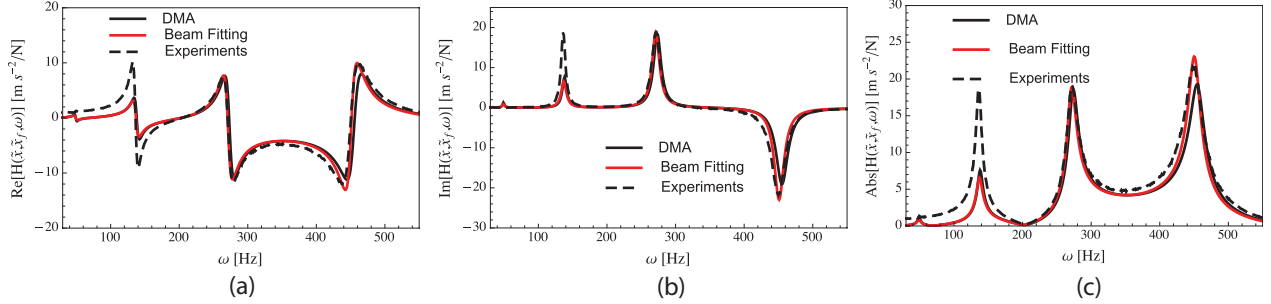


FIG. 11: The comparison between the measured FRF $H_m(\tilde{x}, \tilde{x}_f, \omega)$ (black dashed lines) and the theoretical FRF $H_{th}(\tilde{x}, \tilde{x}_f, \omega)$, obtained through beam-best fitting (red lines) and DMA data (black solid lines), for the beam with $L = 40$ [cm], in the range $30 - 550$ [Hz], in terms of real part (a), imaginary part (b) and absolute value (c) of the FRFs.

IV. RESULTS AND DISCUSSIONS

The first experimental data set considered is related to the beam with $L = 60$ [cm]. From the first iterations, we found that, in order to obtain the best results, it is preferable to consider two peaks at a time, i.e. the second and the third resonances in the frequency range $30 - 150$ [Hz] (see Figure 3-a). The best fitting of the theoretical model (Eq.20) has been achieved by means of 11 relaxation times, and it is shown in Figure 5, where the measured FRF $H_m(\tilde{x}, \tilde{x}_f, \omega)$ (black dashed lines) is compared with the theoretical FRFs $H_{th}(\tilde{x}, \tilde{x}_f, \omega)$, obtained by utilizing Eq.(19), and by considering the viscoelastic modulus calculated by means of both the beam-fitting procedure (red lines) and the DMA-fitted data (black solid lines), in terms of real part (a), imaginary part (b) and absolute value (c) of the FRFs. Interestingly, it is possible to observe a very good overlapping between the measured curves and the theoretical FRF obtained with our proposed method. The viscoelastic modulus $E(\omega)$ calculated by minimizing the cost function ϵ_k Eq.20 is shown in Figure 6 (dashed lines), where it is compared with the viscoelastic modulus measured with DMA (solid lines), in the frequency range $30 - 150$ [Hz].

The higher frequency range, i.e. $150 - 500$ [Hz], has been studied by investigating the dynamic response of the beam with smaller length, i.e. $L = 40$ [cm]. In this case, we obtained the best fit with 8 relaxation times. Let us notice that, despite of the broader frequency range now considered, the number of relaxation times in this case is less than that

one utilized in the previous case (i.e. 11 relaxation times). The reason is probably related to the fact that the transition region of LUBRIFLON is found at low frequency (see Figure 4-b), and therefore the more the frequencies are low, the more the viscoelastic modulus must be characterized through a higher number of relaxation times to properly describe the fast increase of damping, i.e. of the imaginary part $\text{Im}[E(\omega)]$. In Figure 7, we compare the measured FRF $H_m(\tilde{x}, \tilde{x}_f, \omega)$ (black dashed lines) with the theoretical FRFs $H_{th}(\tilde{x}, \tilde{x}_f, \omega)$ (Eq.(19)), calculated by considering the viscoelastic modulus experimentally obtained by means of the beam dynamics (red lines) and through DMA (black solid lines), in terms of real part (a), imaginary part (b) and absolute value (c) of the FRFs. Also in this case, the proposed approach turns out to be very suitable for the viscoelastic material characterization. Indeed, it is possible to observe in Figure 8 a good overlapping, in the frequency range 150 – 550 [Hz], between the viscoelastic moduli $E(\omega)$ experimentally obtained by DMA (solid lines), and by the proposed approach (dashed lines), both for the real part (Figure 8-a) and the imaginary part (Figure 8-b).

At last, the viscoelastic moduli $E(\omega)$, characterized by means of the vibrational analysis on the beams with lengths $L = 60$ [cm] (30 – 150 [Hz]) and $L = 40$ [cm] (150 – 550 [Hz]), previously shown respectively in the Figures 6-8, have been fitted through Eq.(2) in the whole frequency range 30 – 550 [Hz]. In Figure 9, we show the viscoelastic modulus $E(\omega)$ determined by means of the beam dynamics (dashed lines) and the one measured with DMA (solid lines). For both the real part (Figure 9-a) and the imaginary part (Figure 9-b) of the viscoelastic modulus $E(\omega)$, we obtained a fine matching, thus finally assessing the method proposed in this paper. In Figure 10, we compare, in the range 30 – 550 [Hz], the measured FRF $H_m(\tilde{x}, \tilde{x}_f, \omega)$ (black dashed lines) with the theoretical curves $H_{th}(\tilde{x}, \tilde{x}_f, \omega)$, obtained through the so calculated viscoelastic modulus $E(\omega)$ (Figure 9) (red lines) and by means of DMA data (black solid lines), for the beam with $L = 60$ [cm]. It is important to highlight that the two theoretical FRFs $H_{th}(\tilde{x}, \tilde{x}_f, \omega)$ are overlapped in all the frequency range, while the experimental FRF follows the theoretical curves only in the range 30 – 150 [Hz], where we obtained maximum coherence (see Figure 3-a). The "non-detected peak" at 300 [Hz] in the experimental acquisitions, is strictly related to the drop in the coherence function, and could be the origin of the non perfect overlapping between the theoretical and experimental FRFs in the range 150 – 550 [Hz].

Similar reasonings can be made for the results obtained from the beam with $L = 40$ [cm].

In Figure 11 we report the theoretical and the experimental FRFs in this case, where it is evident the good correspondence between the theoretical functions $H_{th}(\tilde{x}, \tilde{x}_f, \omega)$, obtained through our proposed procedure (red lines) and by means of DMA data (black solid lines), in all the frequency range 30 – 550 [Hz]. However, also in this case, the experimental curve follows the theoretical ones in a limited range, i.e. 200 – 550 [Hz], which is far from the presence of a "non-detected peak" at around 65 [Hz] (see Figure 3-b), that probably caused a drop in the coherence function. Moreover, at very small frequencies (~ 10 [Hz]), in both the experimental acquisitions (Figure 3-a,b) it should be observed that coherence tends to decrease below limit values, i.e. < 0.8 , because of the intrinsic problematic of the instrumentations, especially of the impact hammer.

In light of what has emerged from the results shown so far, some remarks should be made, in order to define guidelines for the procedure proposed in this paper. First, we found that for a good fitting of the vibrational response of the beam, the frequency range where coherence is not maximum, as well as some peaks near these areas, should be excluded from the fitting calculations. Furthermore, it has been shown that, the more we proceed towards frequencies where damping is high, i.e. versus the transition zone of the viscoelastic material, the more we need to consider a narrow frequency band to fit the beam response, and an increasing number of relaxation times to describe the viscoelastic modulus $E(\omega)$ is required too.

In conclusion, the proposed method for the characterization of the viscoelastic materials, has revealed to be very efficient, easy to use, and reliable with inexpensive instrumentation. Moreover, the analytical model here presented and used to fit the experimental response of the beam, in particular, has proven to be accurate. The comparison between the viscoelastic moduli $E(\omega)$ characterized by means of our technique and through DMA, indeed, finally assessed the possibility to retrieve this so important mechanical quantity, by simply investigating the dynamics of a viscoelastic beam. We also found that, the idea to consider more beams with different lengths, is very useful to increase the frequency range of interest, and, in principle, by studying the dynamics of even longer or shorter beams, it is possible to cover wider frequency ranges. However, it should be highlighted that in order to obtain a range comparable with the one usually covered by DMA, a different instrumentation should be utilized. In particular, the impact hammer represents a limit in this direction, and it should be substituted with an electrodynamic shaker, which enables to investigate

a wider frequency range maintaining high coherence. At last, also by controlling the surrounding temperature, is possible to enlarge the range of interest, i.e. by a frequency shift of the viscoelastic modulus $E(\omega)$ under study. These last two modifications to the actual experimental setup, will be object of further investigations.

A. Conclusions

In this paper we have presented a very simple and accurate experimental approach for determining the complex modulus of viscoelastic materials. By means of the vibrational behaviour of suspended viscoelastic beams with different lengths, we have characterized the complex modulus of LUBRIFLON by fitting the measured response through an accurate analytical model of the beam dynamics, which takes into account multiple relaxation times of the material. In particular, the possibility to properly select the number of relaxation times in a frequency range of interest, turned out to be a key factor to obtain very good results. The instrumentation utilized in our experiments is inexpensive and easy to use, and it consists of an impact hammer and a suspended beam, instrumented by means of an accelerometer connected to a data acquiring module. Comparisons with DMA measurements demonstrate the validity of the proposed technique on a frequency range which could be comparable with the one usually covered by DMA technique. In conclusion, the proposed procedure represents a valid alternative approach to DMA, and can be considered as a significative step forward the improvement of the mechanical characterization of viscoelastic materials.

-
- [1] Bottiglione F., Carbone G., Mangialardi L., Mantriota G., Leakage Mechanism in Flat Seals, *Journal of Applied Physics* 106 (10), 104902, (2009).
 - [2] Carbone G., Pierro E., Gorb S., Origin of the superior adhesive performance of mushroom shaped microstructured surfaces, *Soft Matter* 7 (12), 5545-5552, DOI:10.1039/C0SM01482F, (2011).
 - [3] Carbone G., Pierro E., Sticky bio-inspired micropillars: Finding the best shape, *SMALL*, 8 (9), 1449-1454, (2012).

- [4] Carbone G., Pierro E., Effect of interfacial air entrapment on the adhesion of bio-inspired mushroom-shaped micro-pillars, *Soft Matter*, 8 (30), 7904-7908, (2012).
- [5] Carbone G., Pierro E., A review of adhesion mechanisms of mushroom-shaped microstructured adhesives, *Meccanica*, 48(8), 1819-1833, (2013).
- [6] Christensen R. M., *Theory of viscoelasticity*, Academic Press, New York.
- [7] Chartoff, R. P., Menczel, J. D. and Dillman, S. H., Dynamic Mechanical Analysis (DMA), in: *Thermal Analysis of Polymers: Fundamentals and Applications* (eds J. D. Menczel and R. B. Prime), John Wiley & Sons, Inc., Hoboken, NJ, USA, 2009.
- [8] Huayamares S., Grund D., Taha I., Comparison between 3-point bending and torsion methods for determining the viscoelastic properties of fiber-reinforced epoxy, *Polymer Testing*, 85 (106428), 2020.
- [9] Nolle A. W., Methods for measuring dynamic mechanical properties of rubber-like materials," *Journal of Applied Physics*, vol. 19, no. 8, pp. 753–774, 1948.
- [10] Nijenhuis K., Survey of measuring techniques for the determination of the dynamic moduli, in *Rheology*, pp. 263–282, Springer, Berlin, Germany, 1980.
- [11] Esmaeeli R., Aliniagerdroudbari H., Hashemi S. R., Jbr C., Farhad S., Designing a New Dynamic Mechanical Analysis (DMA) System for Testing Viscoelastic Materials at High Frequencies, *Modelling and Simulation in Engineering*, Volume 2019, Article ID 7026267, 9 pages.
- [12] Pritz T., Dynamic strain of a longitudinally vibrating viscoelastic rod with an end mass, *Journal of Sound and Vibration* 85 (2), 151–167, 1982.
- [13] Trendafilova I.N., Odeen S., Lundberg B., Identification of viscoelastic materials from electro-optical displacement measurements at two sections of an impacted rod specimen, *European Journal of Mechanics A: Solids* 13 (6),793–802, 1994.
- [14] Casimir J.B., Vinh T., Measuring the complex moduli of materials by using the double pendulum system, *Journal of Sound and Vibration* 331 (6), 1342–1354, 2012.
- [15] Cortes F. , Elejabarrieta M.J., Viscoelastic materials characterisation using the seismic response, *Materials and Design*, 28, 2054–2062, (2007).
- [16] Inman D. J., *Engineering Vibrations*. Upper Saddle River, NJ: Prentice Hall, 1996.
- [17] Pierro E., Viscoelastic beam dynamics: Theoretical analysis on damping mechanisms, in: *7th International Conference on Computational Methods in Structural Dynamics and Earthquake Engineering*, COMPDYN 2019, Crete, Greece, 24 June, pp. 4396-4407, 2019.

- [18] Pierro E., Damping control in viscoelastic beam dynamics, *Journal of Vibration and Control*, doi: 10.1177/1077546320903195.
- [19] <https://www.dixon-resine.it/>
- [20] D. J. Ewins, *Modal Testing: Theory, Practice and Applications*, Taunton: Research Studies Press, 1984.
- [21] Pintelon R. and Schoukens J., *System Identification: A Frequency Domain Approach*, IEEE Press, Piscataway, NJ, USA, 2001.